Electronic Supplementary Material (ESI) for Materials Chemistry Frontiers.

Supporting Information

Graphene oxide co-doped with dielectric and magnetic phases as electromagnetic wave suppressor

Sourav Biswas[a], Yudhajit Bhattacharjee[b], Sujit S Panja[a*], Suryasarathi Bose[b*]

[a] Department of Chemistry, National Institute of Technology Durgapur-713209, West Bengal, India.
[b] Department of Materials Engineering, Indian Institute of Science, Bangalore- 560012, Karnataka, India.
* Author to whom all the correspondence should be addressed.
Email: sujit.panja@gmail.com (SP) ; sbose@materials.iisc.ernet.in (SB)

Table of content

	Contents		Figure /Table No.
1.	Preparation of PC nanocomposite	……	S1
2.	UV-Vis spectra of washed solution	……	S2
3.	EDS analysis of MDA modified BT/Fe co-doped GO nanoparticles	……	S3
4.	DSC experiments of blends	……	S4
5.	Mechanical properties of blends	……	S5
6.	Complex permittivity and permeability	……	S6
7.	Absorption and reflection percentage	……	S7
8.	Magneto-dielectric study	……	S8
9.	Synergetic effect of absorption	……	S9
10.	Impedance matching	……	S10
11.	Parameters obtained from power law fitting	……	T1
12.	Total shielding effectiveness of various shield materials with different thickness	……	T2
13.	EM shielding performances of various PVDF and PC based matrix with MWCNTs and/or GO as filler nanoparticles	…….	T3

Preparation of PC nanocomposite via nucleophilic substitution reaction:

Previously synthesized MDA modified BT/Fe co-doped GO nanoparticles were sonicated and mixed with PC with required amount of the blend composition and then treated at 150°C in DMF solution 24h. The resultant mixture was then poured in a Teflon coated petri dish for solvent evaporation. Finally the sheets were vacuum dried and used as PC nanocomposite. During the reaction carbonyl groups of PC can undergo a nucleophilic substitution reaction with the amine terminated end of MDA.

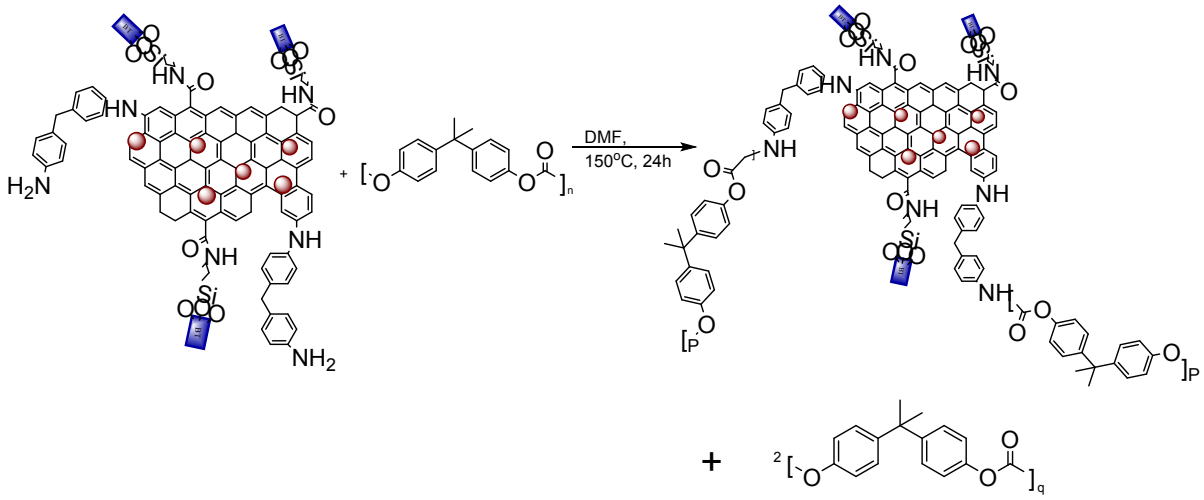

Figure S1: Schematic representation showing the preparation of PC/MDA modified GO nanocomposites.

Removal of un-bound ACA molecules from the MWCNT-ACA

Antharacene based ACA has a very strong interaction with MWCNTs due to π-π stacking originated from extended π-conjugation of antharacene moiety and delocalized π-cloud in MWCNTs. So surface of MWCNTs were modified here by non-covalent attachment of ACA molecules in a typical weight ratio of 2:1. After completion of the attachment process the unbound ACA molecules were removed by washing with sufficient amount of solvent several times. UV-Vis spectra of solvent generally guided us for the complete removal of ACA molecules after 6th wash.

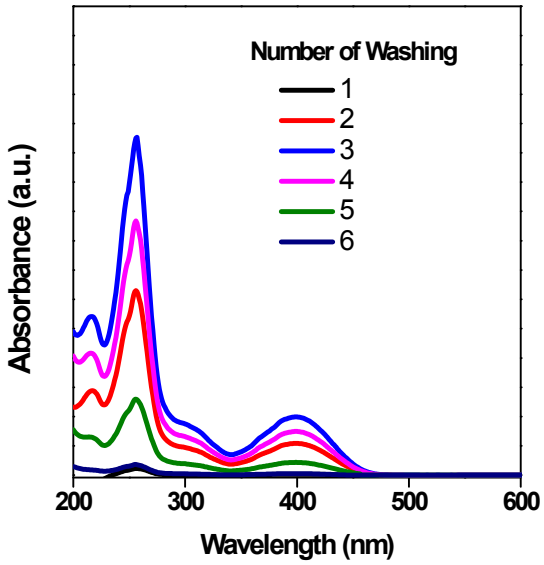

Figure S2: UV-Vis spectra obtained after different washing cycles.

EDS analysis of MDA modified r-GO/BT/Fe nanoparticles:

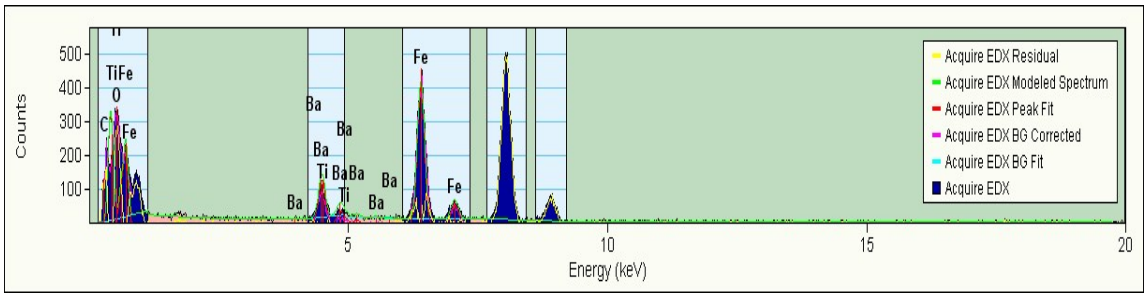

Figure S3: EDS analysis of MDA modified BT/Fe co-doped GO *nanoparticles*

Tailor-made localization of nanoparticles: assessing by DSC study

Generally the crystallization behavior is one of the key factors that dictate the structural performance of the blend structure, more specifically when one of the components of the blend is semi crystalline polymer like PVDF. The presence of any external rigid nanoparticles and their distribution inside the blend can affect this crystallization behavior greatly. It is observed that when the MWCNTs are selectively localised at PVDF the crystallization and melting temperatures of PVDF has increased. This is mainly because MWCNTs are acting as hetero nucleating agent. But interestingly after addition of ACA modified MWCNTs

enhancement in crystallization and melting temperature is further modified due to extent of better exfoliation of MWCNTs into the PVDF. Further enhancement is observed after incorporation of MDA modified BT/Fe co-doped GO into the PVDF. But after tailor-made localization of this nanoparticle into the PC such enhancement is not observed.

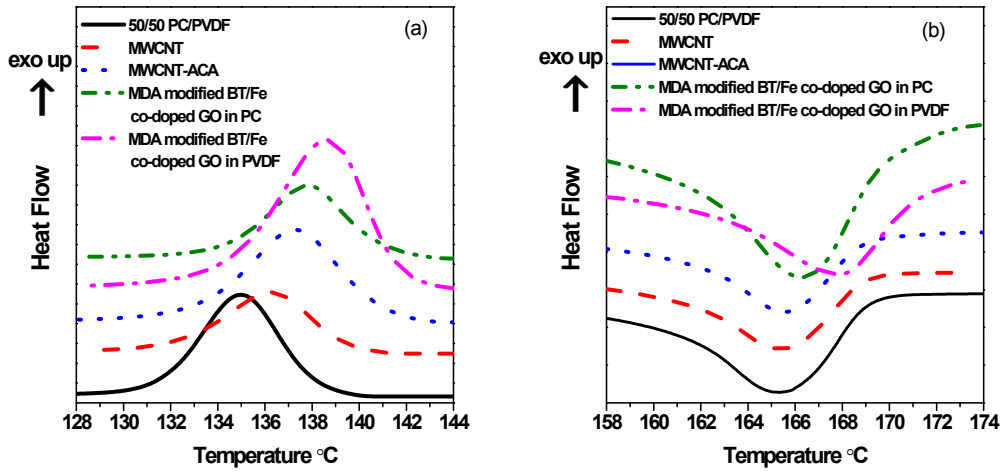

Figure S4: DSC (a) crystallization temperature, (b) melting temperature of various samples

Mechanical properties:

Interfacial adhesion between the constituent polymers is the prime factor on deciding the mechanical properties of the blend system. After incorporation of MWCNTs into the blend an improvement in tensile property and in Young's modulus is observed. But elongation at break is poor stress transfer at the interfacial region leads to immature failure. However after addition of ACA modified MWCNTs into the blend a slight improvement in overall mechanical properties are observed due to better exfoliation. But a drastic change is observed after addition of MDA modified BT/Fe co-doped GO nanoparticles into the PVDF because of very poor stress transfer at the interfacial region. Such observation is also corroborated with the SEM micrograph, where two distinct phases were observed one is highly coarse and other is smooth. Besides crystallization of PVDF phase also affect the mechanical properties, as poor stress transfer at the interfacial region. But after preferential localization of MDA modified BT/Fe co-doped GO nanoparticles into the PC and MWCNT-ACA at the PVDF a slight improvement is observed.

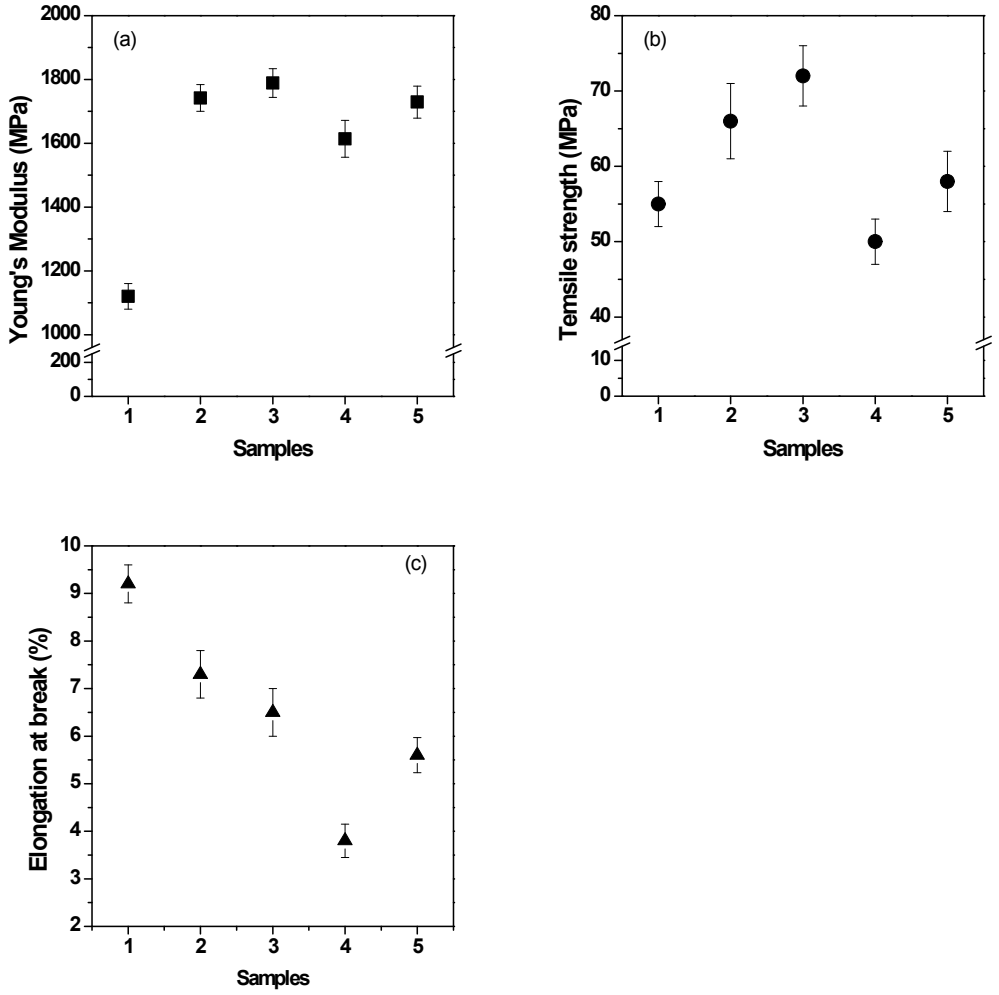

Figure S5: (a) Young's modulus, (b) tensile strength, (c) elongation at break of various samples (where (1) neat PC/PVDF (2) PC/PVDF with MWCNT, (3) PC/PVDF with MWCNT-ACA, (4) PC/PVDF with MWCNT-ACA + MDA modified BT/Fe co-doped GO in PVDF, (5) PC/PVDF with MWCNT-ACA + MDA modified BT/Fe co-doped GO in PC)

Complex permittivity and permeability parameters for various blends

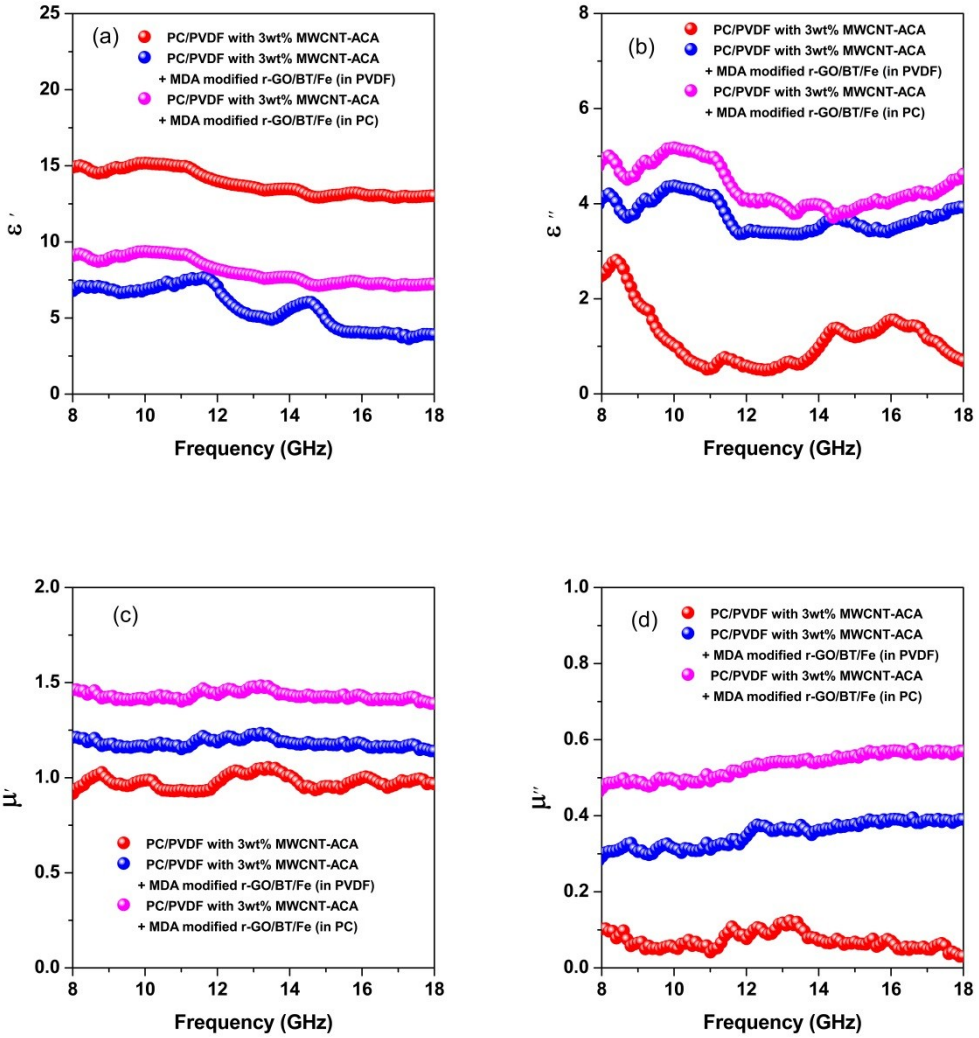

Figure S6: Complex permittivity (a) real part, (b) imaginary part. Complex permeability (a) real part, (b) imaginary part for various blends.

Absorption and reflection coefficient of the total shielding effectiveness

We have estimated the total absorption and reflection component of the total shielding effectiveness in terms of percentage. It is observed that the mechanism of shielding has altered from refection to absorption after co-doping magnetic and dielectric phases. Further enhancement in absorption was facilitated by impedance mismatch.

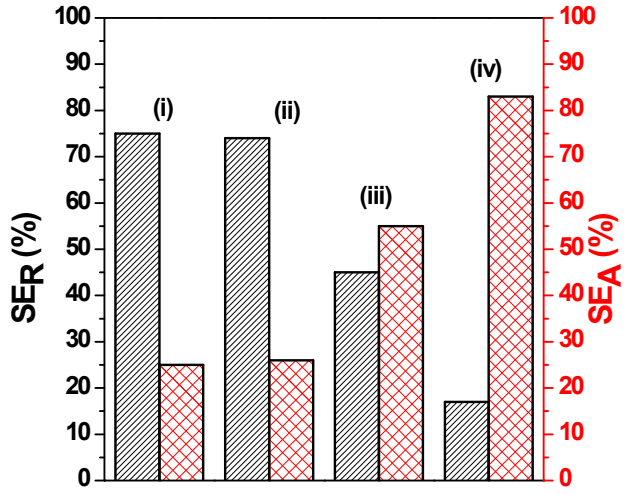

Figure S8: *Absorption and reflection component of various blends (where (i) PC/PVDF with MWCNT, (ii) PC/PVDF with MWCNT-ACA, (iii) PC/PVDF with MWCNT-ACA + MDA modified BT/Fe co-doped GO in PVDF, (iv) PC/PVDF with MWCNT-ACA + MDA modified BT/Fe co-doped GO in PC)*

Magneto-capacitance measurement

Figure S8 shows the variation in magneto-capacitance (MC) as a function of magnetic field varied from 0 to 10000 Oe at 1000 Hz. MC can be defined as,

$$\text{MC} = \frac{\varepsilon\,(H) - \varepsilon\,(0)}{\varepsilon\,(0)} x100$$

where ε (H) and ε (0) are the dielectric constant in presence and absence of magnetic field respectively. The change in the dielectric constant on varying the magnetic field is due to magnetostriction effect, which occurs due to change in lattice parameters. If we apply magnetic field to a magnetoelelctric material, the material gets strained, and this strain further induces stress which gives rise to an electric field. This generated field is able to orient the ferroelectric domains, and hence dielectric behavior is altered. So here magneto-capacitance suggests that our synthesized materials have magento-dielectric property. More interestingly the value of magneto capacitance is quite impressive in our case when compared to the available literature. Macroscopic inhomogeneities can have surprising impact on magnetotransport of a material. It is envisaged that materials can exhibit magnetic-field-

dependent dielectric response without any magnetism. Our nanocomposites showed a magneto-capacitance effect with the dielectric constant changing by 10% as the magnetic field was increased to 1 T. This effect was explained as arising because of MaxwellWagner polarization as applied to inhomogeneous materials.

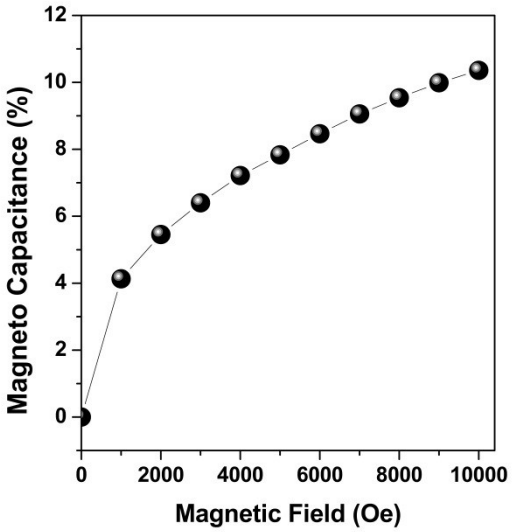

Figure S8: Magneto-capacitance of MDA modified BT/Fe co-doped GO particles

Synergetic effect of permittivity and permeability parameters

Figure S9 exhibits that higher dielectric/magnetic loss and lower dielectric permittivity/permeability will facilitate in higher impedance matching. The MWCNT-ACA containing blend was compared here with MWCNT-ACA + MDA modified BT/Fe co-doped GO in PC phase.

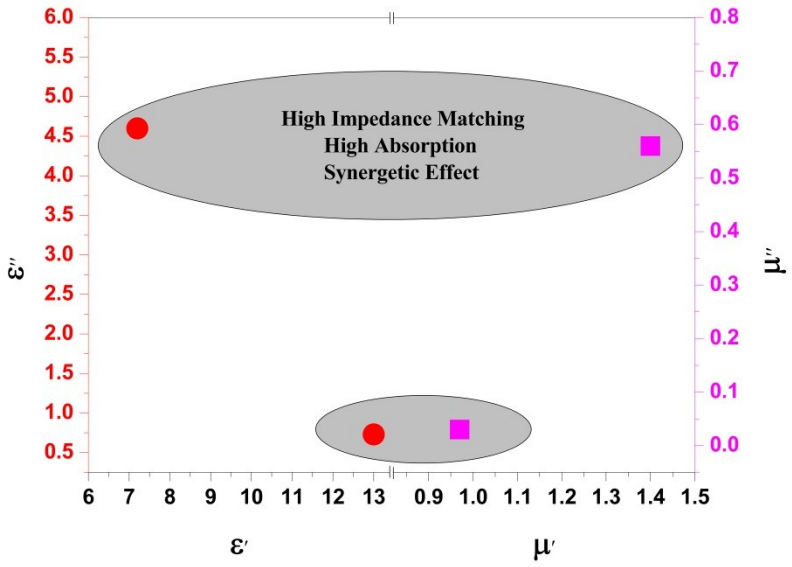

Figure S9: Synergetic effect leading to impedance matching in various blends.

Impedance matching of blends structures

Figure S10 compares the ratio of real part of the permittivity and permeability as a function of frequency for different blends investigated here.

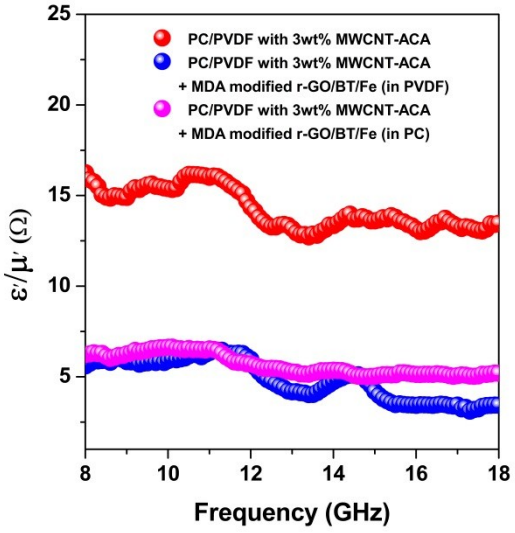

Figure S10: Impedance matching in various blends

Table T1: Parameters obtained from power law fitting

Composition	σ_{DC} (S cm^{-1})	Exponent (n)
PC/PVDF with 3wt% MWNT	6.15×10^{-5}	0.74
PC/PVDF with 3wt% MWNT-ACA	0.985×10^{-2}	0.68
PC/PVDF with 3wt% MWNT-ACA + MDA modified BT/Fe co-doped GO (both in PVDF)	1.12×10^{-9}	0.89
PC/PVDF with 3 wt% MWNT-ACA + MDA modified BT/Fe co-doped GO (in PC)	2.46×10^{-6}	0.71

Table T2: Total shielding effectiveness of various shield materials with different thickness

Composition	Thickness (mm)	SE_T (dB)
PVDF with 3wt% MWCNT	0.9	-9
PC with 3wt% MWCNT	0.9	-8
PC/PVDF with 3wt% MWCNT	0.9	-16
	0.3	-12
PC/PVDF with 3wt% MWCNT-ACA	0.9	-19
	0.3	-14
PC/PVDF with 3wt% MWCNT-ACA + MDA modified BT/Fe co-doped GO (both in PVDF)	0.9	-22
	0.3	-15
PC/PVDF with 3 wt% MWCNT-ACA + MDA modified BT/Fe co-doped GO (in PC)	0.9	-34
	0.3	-26
PC/PVDF + MDA modified BT/Fe co-doped GO (in PVDF)	0.9	-3
PC/PVDF + MDA modified BT/Fe co-doped GO (in PC)	0.9	-2
Multilayer assembly 1 [PVDF with 3wt% MWCNT-ACA (in upper and bottom layer) PC/PVDF with 3 wt% MWCNT-ACA + MDA modified BT/Fe co-doped GO (in PC) (middle layer)]	0.9	-30
Multilayer assembly 2 [PVDF with 3wt% MWCNT-ACA (middle layer) PC/PVDF with 3 wt% MWCNT-ACA + MDA modified BT/Fe co-doped GO (in PC) (in upper and bottom layer)]	0.9	-46

Table T3: EM shielding performances of various PVDF and PC based matrix with MWCNTs and/or GO as filler nanoparticles

Matrix	Nanoparticles	Thickness (mm)	Frequency (GHz)	SE_T (dB)	
PVDF	f-GO (5 wt%)	-	8-12	-20	[1]
PVDF	f-MWCNT (2wt%)	5	8-18	-20	[2]
PVDF	f-MWCNT (1wt%) MNT (5 wt%)	-	8-12	-20	[3]
PVDF	MWCNT (3wt%) Co nanowire (5 wt%)	5	8-18	-35	[4]
PVDF	MWCNT (3wt%) NiFe (50wt%)	6	8-18	-35	[5]
PVDF	f-MWCNT (0.5 wt%)	-	12-18	-38	[6]
PVDF/PMMA/ PTFE	CNF	-	8.2-12.4	-25	[7]
PC	MWCNT (15 wt%)	2	8-12	-26	[8]
PC/SAN	GO-Ni (5 wt%)	5	8-18	-29	[9]
PC/PVDF	MWCNT-AHB-Fe3O4	0.9	12-18	-31	[10]
PC/PVDF	MWCNT (3 wt%) BT (5wt%)	5	8-18	-38	[11]
PC/PVDF	IL-MWCNT (3 wt%) BaFe (5wt%)	5	8-18	-37	[12]
PC/PVDF	MWCNT-ACA (3wt%) MDA modified BT/Fe co-doped GO (5 wt%)	0.9	8-18	-34	This work
PC/PVDF multi-layer assembly	MWCNT-ACA (3wt%) MDA modified BT/Fe co-doped GO (5 wt%)	0.9	12-18	-46	This work

References:

1. V. Eswaraiah, V. Sankaranarayanan and S. Ramaprabhu, *Macromol. Mater. Eng*, 2011, **296**, 894-898.
2. M. Sharma, S. Sharma, J. Abraham, S. Thomas, G. Madras and S. Bose, *Mater. Res. Express*, 2014, **1**, 035003.
3. V. Eswaraiah, V. Sankaranarayanan and S. Ramaprabhu, *Nanoscale Res. Lett.*, 2011, **6**, 1-11.
4. M. Sharma, M. P. Singh, C. Srivastava, G. Madras and S. Bose, *ACS Appl. Mater. Interfaces*, 2014, **6**, 21151-21160.
5. V. Bhingardive, S. Suwas and S. Bose, *RSC Adv.*, 2015, **5**, 79463-79472.
6. G. S. Kumar, D. Vishnupriya, A. Joshi, S. Datar and T. U. Patro, *Phys. Chem. Chem. Phys.*, 2015, **17**, 20347-20360.

7. A. Das, H. T. Hayvaci, M. K. Tiwari, I. S. Bayer, D. Erricolo and C. M. Megaridis, *J. Colloid Interface Sci.*, 2011, **353**, 311-315.
8. M. Arjmand, M. Mahmoodi, G. A. Gelves, S. Park and U. Sundararaj, *carbon*, 2011, **49**, 3430-3440.
9. S. P. Pawar, S. Stephen, S. Bose and V. Mittal, *Phys. Chem. Chem. Phys.*, 2015, **17**, 14922-14930.
10. S. Biswas, S. S. Panja and S. Bose, *Materials Chemistry Frontiers*, 2017.
11. S. Biswas, G. P. Kar and S. Bose, *Nanoscale*, 2015, **7**, 11334-11351.
12. S. Biswas, G. P. Kar and S. Bose, *ACS Appl. Mater. Interfaces*, 2015, **7**, 25448-25463.